Lateral phase separation in tense membranes

Tsutomu Hamada,*[a] Yuko Kishimoto,[a] Takeshi Nagasaki[b] and Masahiro Takagi[a]

Received (in XXX, XXX) Xth XXXXXXXXX 200X, Accepted Xth XXXXXXXXX 200X
First published on the web Xth XXXXXXXXX 200X
DOI: 10.1039/b000000x

The organization of lateral domains, called lipid rafts, in plasma membranes is essential for physiological functions, such as signaling and trafficking. In this study, we performed a systematic analysis of lateral phase separation under membrane tension. We applied osmotic pressure directed toward the outside of vesicles to induce membrane tension. Microscopic observations clarified the shifts in phase structures within bilayer membranes with change in tension and temperature. The miscibility transition temperature between one-liquid and two-liquid states was shown to increase under tension. We also observed a shift in the transition temperature between two-liquid and solid-liquid states in membranes under tension. We determined a quantitative phase diagram of phase organization with respect to the applied pressure and temperature. The results indicate that membrane tension can induce phase separation in homogeneous membranes. Our findings may provide insight into the biophysics of bilayer phase organization under tension, which is an intrinsic mechanical property of membranes.

Introduction

The organization of lateral membrane structure is essential for physiological functions.[1] Within two-dimensional fluid membranes, microdomains called lipid rafts, which are composed largely of cholesterol and saturated lipids, are laterally segregated with high lipid order and slow dynamics.[2,3] During molecular-associating events at a membrane interface, such as signaling and trafficking, stabilized microdomains are produced to effectively concentrate specific molecules. Recently, much attention has been given to understanding the biophysical mechanism of the formation of microdomains.[4] Membrane lateral domains are considered to be a form of two-dimensional phase separation that develops due to the interaction between lipid molecules.[1,5] To reveal the physicochemical properties of membrane microdomains, several studies have considered model membrane systems using multi-component lipid vesicles.[6-9] Microscopic observations have revealed that vesicles that are simply composed of saturated and unsaturated lipids together with cholesterol show phase separation into domains under specific conditions.[10] With regard to thermodynamic phase separation, the stability of lipid bilayer miscibility, such as the emergence of raft domains, should be determined by physical variables such as temperature, the mixing fraction, and lateral pressure. At high temperature, membranes are in a one-liquid phase due to the large effect of mixing entropy, and a decrease in temperature induces a phase separation between ordered and disordered phases.[10] The phase diagram with regard to the mixing fraction of the constituent molecules has also been well characterized; phase separation such as two-liquid and solid-liquid organization was observed depending on the proportions in a ternary lipid mixture.[11] Along these lines, we also reported that a change in the conformation of a membrane-constituting molecule can switch the membrane lateral organization in a reversible manner.[12]

Even under a constant temperature and mixing fraction, the thermodynamic phase behavior of membranes should also be affected by another variable, such as lateral pressure.[13] The equation of state concerning lateral pressure and molecular area has been thoroughly studied in lipid monolayer membranes, since it is possible to control the area-per-lipid using a Langmuir trough.[14] Conversely, there has been no systematic study of bilayer phase organization under lateral pressure. This is attributed to the difficulty of controlling lateral pressure in bilayer vesicles. In bilayer membranes, lateral pressure balances the lipid-water interfacial tension, where lipid molecules have a fixed molecular area.[15] However, external mechanical forces, such as osmotic pressure, shear stress and adhesion, can stretch the bilayer membrane, which leads to a change in the balance of forces within the bilayer. Such modulation under mechanical forces is generally described as membrane tension, which is a function of the change in area-per-lipid.[16] Very recently, some reports have addressed the stabilization of laterally-segregated domains with regard to membrane tension. Rozovsky et al., reported the transformation of domain shapes from stripes to circles in adhering vesicles with a ternary mixture of sphingomyelin, unsaturated lipid and cholesterol.[17] Komura et al., theoretically suggested that the pertinent mechanism can be attributed to an enhanced membrane surface tension that is induced by vesicle adhesion onto a solid surface.[18] Li and Cheng also reported that membrane tension can affect the shape of domains in binary vesicles composed of saturated and unsaturated lipids, by reducing membrane tension by adding a negatively charged lipid or by growing vesicles in sucrose solutions.[19] Ayuyan and Cohen reported that membrane tension regulates raft enlargement: the blurring and sharpening of domain edges was observed in a hypoosmotic condition.[20] However, there have been no further systematic experiments on the effect of applied forces on the bilayer phase separation, such as a phase diagram, and there are still

large gaps in our understanding tension-induced lateral phase organization in a lipid bilayer.

In this study, we performed microscopic observations of multi-component giant vesicles to clarify membrane phase behavior of tense membranes. We applied osmotic pressure directed toward the outside of vesicles to induce membrane tension. Membrane tension σ is described as

$$\sigma = \frac{pr}{2} + \frac{\kappa c_0}{2r}(2 - c_0 r) \qquad (1)$$

where p is the osmotic pressure between inner and outer media, r is the radius of vesicles, κ is the bending modulus, and c_o is the spontaneous curvature.[21] We obtained a quantitative phase diagram of lateral membrane organization for an applied pressure and temperature. Membrane tension induces changes in membrane phase organization: under tension, one-liquid membranes tend to show lateral phase separation into domains, and two-liquid vesicles change their structure to a solid-liquid organization.

Experimental

Materials

Dioleoyl L-α phosphatidylcholine (DOPC), dipalmitoyl L-α phosphatidylcholine (DPPC), and cholesterol (Chol) were obtained from Avanti Polar Lipids (Alabaster, AL). N-(Rhodamine red-X)-1,2-dihexadecanoyl-sn-glycero-3-phosphoethanolamine triethylammonium salt (rho-PE, λ_{ex} = 560 nm, λ_{em} = 580 nm) was obtained from Invitrogen (Carlsbad, CA). D(+)-Glucose was purchased from Nacalai Tesque (Kyoto, Japan). Bis[N,N-bis(carboxymethyl)-aminomethyl]fluorescein (calcein) was obtained from Wako Pure Chemical Industries (Osaka, Japan). Deionized water was obtained using a Millipore Milli Q purification system.

Preparation of multi-component giant vesicles

Giant vesicles were prepared using the natural swelling method from a dry lipid film:[22] the lipid mixture dissolved in 2:1 (v/v) chloroform/methanol along with rho-PE in a glass test tube were dried under vacuum for 3 h to form thin lipid films. Next, the films were hydrated with 200mM glucose solution at 37 °C for several hours. The final concentrations were 0.2 mM lipids (DOPC/DPPC/Chol) with 0.5 mol % rho-PE.

Microscopic observation under osmotic stress

The prepared vesicle solution was incubated for more than half an hour at 40 °C (above the miscibility transition temperature).[10] To introduce the desired osmotic pressure, the solution was then poured into a test tube with some volume of deionized water (warmed at 40 °C) and gently mixed using vortex for 30 s. The solution was placed on a glass coverslip, which was covered with another smaller coverslip at a spacing of ca. 0.1 mm. We observed phase-separated structures in the vesicle surface with a fluorescent microscope (IX71, Olympus, Japan). A standard filter set (U-MWIG3: ex 530-550 nm, dichroic mirror 570 nm, em 575 nm) was used to monitor the fluorescence of rho-PE. The temperature (±0.1°C) of the samples was managed with a microscope stage (type 10021, Japan Hitec). The observation was started after the sample had rested on the stage for 5 min at the desired temperature to permit the formation of microscopic phase-separated domains.

Detection of the penetration of calcein across membranes

By replacing deionized water with calcein solution, we prepared a vesicle solution with calcein (36 μM) only outside the vesicular space under osmotic stress (Δc = 180 mM). As a control, tensionless vesicles with the same calcein gradient across membranes were also prepared; Δc = 0 mM and 36 μM calcein outside the vesicles. The samples were observed by microscopy by the same procedure as described above. A standard filter set (U-MNIBA3: ex 470-495 nm, dichroic mirror 505 nm, em 510-550 nm) was used to monitor the fluorescence of calcein.

Results

Lateral membrane phase separation

Figure 1A shows a phase diagram of ternary vesicles consisting of DOPC/DPPC/Chol at 20 °C. The membrane phase of this system can mainly be classified into three states, one-liquid, two-liquid, and solid-liquid, depending on the mixing fraction of the lipids.[11] Many experimental studies have been conducted to analyze the phase state of membranes, and the equilibrium phase diagrams of ternary vesicles are relatively well characterized.[7]

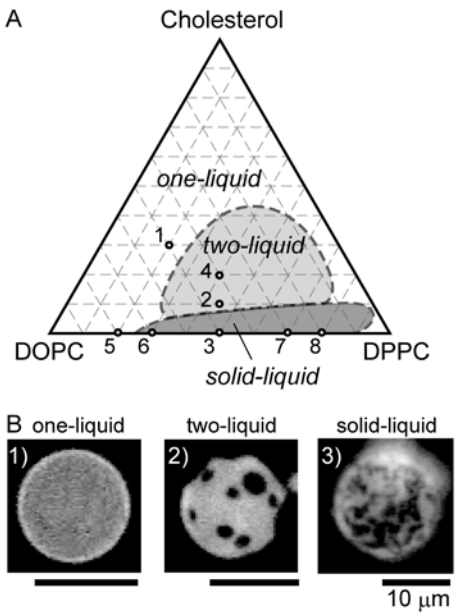

Fig. 1. (A) Typical phase diagram of ternary (DOPC/DPPC/Chol) membranes at 20 °C. Note that the phase boundary is only schematic. Adapted from Ref. 11. (B) Microscopic images of ternary membranes with each thermodynamic phase state: (1) one-liquid with DOPC/DPPC/Chol=50/20/30, (2) two-liquid with DOPC/DPPC/Chol=45/45/10, and (3) solid-liquid with DOPC/DPPC/Chol=50/50/0, which correspond to composition 1, 2 and 3 as shown in part (A).

Typical fluorescent images of the membrane surface under each phase organization are shown in Fig. 1B: DOPC/DPPC/Chol=50/20/30 for one-liquid phase, DOPC/DPPC/Chol=45/45/10 for two-liquid phase, and DOPC/DPPC/Chol=50/50/0 for solid-liquid phase. There is a clear difference in domain structures between two-liquid and solid-liquid phase separations. Liquid domains show circular shapes due to line tension (Fig. 1B-2), while the boundary structure of solid domains is random (Fig. 1B-3). The smoothness of the boundary lines between two phases is a typical characteristic that can be used to identify organized phases by microscopic observations.

Transition from one-liquid to two-liquid phase organization under tension

To obtain tense vesicles, we applied osmotic pressure from inside the membranes (Fig. 2). After the application of osmotic pressure, water efflux across the membrane increases the inner aqueous volume. Thus, the vesicles achieve a completely spherical shape with a maximum volume per area. Further influx then stretches the membranes, i.e., the membranes become under tension. First, we investigated the effect of pressure on a ternary mixture of DOPC/DPPC/Chol=50/20/30 (composition 1 from Fig. 1A), where the membrane is one-liquid without domains at 20 °C (Fig. 3A). After the application of osmotic pressure, phase-separated two-liquid vesicles with domains were produced (Fig. 3B). Figure 4A shows the probability of vesicles with each phase (one-liquid, two-liquid and solid-liquid) as a function of the applied osmotic pressure Δc at 20 °C. The number of vesicles observed for each condition is n=120, which reflects that the experiments were performed three times with n=40. Notably, we counted nearly equal-sized vesicles with a diameter of ~10 μm, since membrane tension changes with the size of vesicles according to eq (1). Without pressure (Δc = 0), almost all of the vesicles show a homogeneous one-liquid phase. As the pressure increased, the number of phase-separated vesicles with domains increased. Solid-liquid phase separation appeared over Δc = 160 mM, and there were no one-liquid vesicles at Δc = 180 mM. Figure 4B shows the probability of phase-separated vesicles as a function of temperature under an osmotic pressure of Δc = 180 mM. The miscibility temperature of this system is T ~ 25 °C, where around half of the vesicles (55 %) show phase separation. At a temperature of 20 °C, the surfaces of all vesicles are covered with liquid (63 %) or solid (37 %) domains. As the temperature decreased, the percentage of solid-liquid phase separation increased. In contrast, when the temperature increased to 30 °C, membranes became homogeneous without domains.

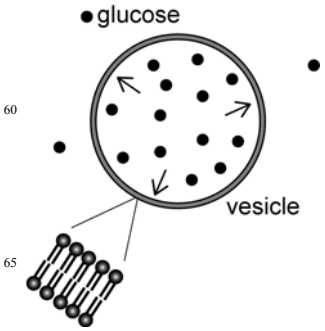

Fig. 2. Schematic representation of a tense vesicle under osmotic pressure with glucose.

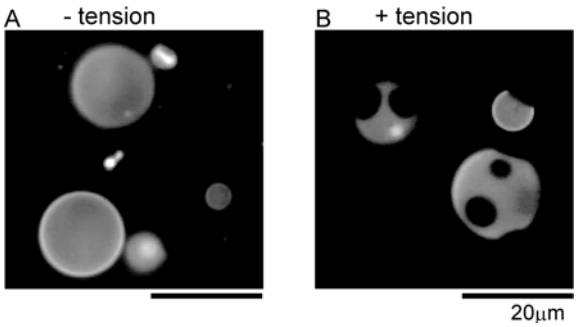

Fig. 3. Tension-induced transition from one-liquid to two-liquid phase organization. Typical microscopic images of tensionless (A) and tense (B) ternary vesicles of DOPC/DPPC/Chol=50/20/30 at 20 °C. Tense vesicles were under an osmotic pressure of Δ*c*=160mM.

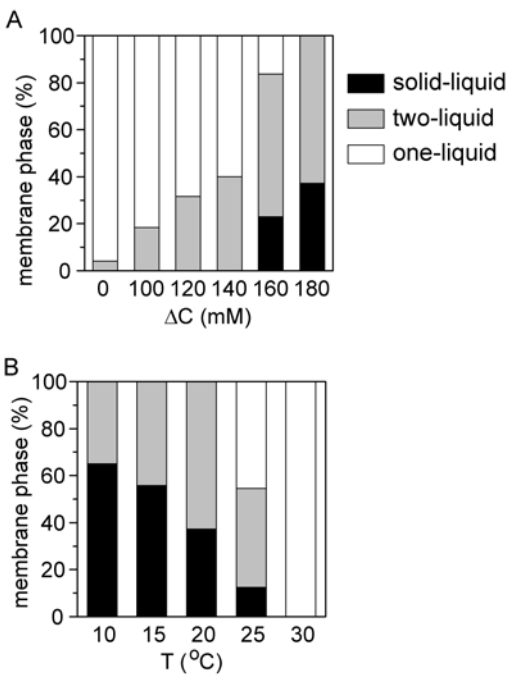

Fig. 4. Probability of phase-separated vesicles of a ternary (DOPC/DPPC/Chol=50/20/30) system; (A) as a function of applied osmotic pressure Δ*c* at 20 °C, and (B) as a function of temperature *T* under an osmotic pressure of Δ*c*=180mM. White, gray and black boxes indicate one-liquid, two-liquid and solid-liquid vesicles, respectively. The

vesicles were left for 5 min at the desired temperature to equilibrate. A total of 120 vesicles were observed for each condition.

We then determined the phase diagram of the lateral organization of ternary DOPC/DPPC/Chol=50/20/30 vesicles as a function of the applied osmotic pressure and temperature (Fig. 5, also see the Supplementary Information). The pressure P is calculated by Van't Hoff's equation $P = RT\Delta c$, where R is the gas constant. We classified the membrane phase state into three categories: >50 % vesicles are in a one-liquid state (cross), or a two-liquid (open circle) or solid-liquid (filled square) state is dominant among two-phase vesicles when ≥50 % vesicles show phase separation. The miscibility temperature increased with an increase in the applied osmotic pressure; the miscibility temperature for Δc = 160 and 180 mM is above 25 °C, which is higher than 15~20 °C for $\Delta c \leq$ 140 mM. Therefore, when the temperature is appropriately chosen to be between the shifts of miscibility temperature, such as 20~25 °C, tension induces membrane phase separation, as shown in Fig. 3. In addition, at low temperature (10 and 15 °C), the application of high osmotic pressure (Δc = 180 mM) resulted in the emergence of solid domains (solid-liquid phase organization). To describe the phase diagram, we did not use tension calculated by eq (1), but rather used experimentally applied osmotic pressure, since there is some experimental dispersion of actual tension on the membranes. The dispersion of lateral tension is attributed to differences in the size of vesicles as eq (1), and also in the area-to-volume ratio of vesicles before osmotic imbalance was applied. During vesicle preparation, vesicles with different area-to-volume ratio (called reduced volume) are spontaneously produced through the gentle hydration method.[23-26] Said differently, the vesicles are not always initially spherical, and rather assume various shapes such as prolate, oblate and stomatocyte. After the application of osmotic pressure, such non-spherical vesicles first become spherical through the influx of water. During this transformation, the glucose concentration in the vesicular space should decrease, and eventually the resulting spherical vesicle is under a smaller osmotic pressure.

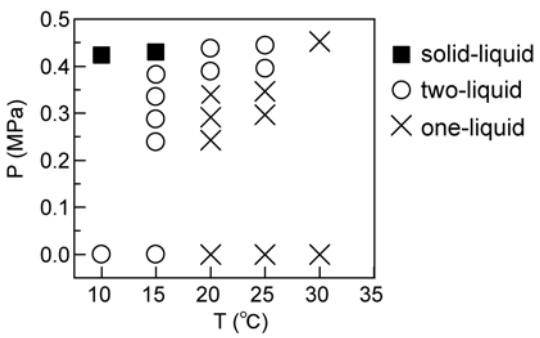

Fig. 5. Phase diagram of membrane lateral organization for applied osmotic pressure P and temperature T. Vesicles are composed of DOPC/DPPC/Chol=50/20/30. The open circles and filled squares correspond to the situation where two-liquid or solid-liquid phase separation is dominant when ≥50 % vesicles show phase separation. Crosses indicate that >50 % vesicles are in the one-liquid (homogenous) state.

Transition from two-liquid to solid-liquid phase organization under tension

Next, we investigated the effect of tension on the phase organization in a DOPC/DPPC/Cho=40/40/20 membrane with domains (composition 4 from Fig. 1A). Before the application of osmotic pressure, the membrane is in a two-liquid state, where the phase-separated membrane surface is covered by several circular domains (Fig. 6A). Figure 6B shows typical images of the membrane surface with the application of osmotic pressure. The pattern of the domain structure changed from a circular liquid phase to a non-circular solid phase. Figure 7A shows the probability of phase-separated DOPC/DPPC/Cho=40/40/20 vesicles (one-liquid, two-liquid and solid-liquid) as a function of the applied osmotic pressure Δc. The temperature of the samples is controlled to be 15 °C. Without pressure (Δc = 0), all of the vesicles show two-liquid phase organization. As the pressure is increased over Δc = 120 mM, vesicles with solid domains appear. When Δc = 180 mM, almost all of the vesicles (98 %) are in a solid-liquid state. Figure 7B shows the probability of phase-separated vesicles as a function of temperature under an osmotic pressure of Δc = 180 mM. At a low temperature below 15 °C, the membrane surfaces of almost all of the vesicles are covered by solid domains. As the temperature is increased over 20 °C, two-phase vesicles with liquid domains increase. The miscibility temperature of this system is ~34 °C, and the one-liquid membrane is dominant (98 %) at 36 °C.

Next, we performed the real-time monitoring of a change in the phase structure of a single vesicle with a change in temperature (Fig. 8). First, the vesicle was situated in the solid-liquid state under an osmotic pressure of Δc = 180 mM at 15 °C, and then we increased the temperature at 10 °C/min. As the temperature increased, the structure of the domains changed into a circular shape, indicating that the vesicle showed phase transition from a solid-liquid to two-liquid state. Thereafter, the area of the domains decreased, and they eventually disappeared. Thus, the vesicles assumed a one-liquid phase. Once a one-phase vesicle was obtained, we again decreased the temperature. Small domains appeared in the membrane surface, and collided into a larger domain.[27] The behavior of domain growth should depend on the phase state of the domains, such as liquid or solid. When the temperature decreased to around 15 °C, the fused domains could not assume a circular shape, indicating that the vesicle reverted to the solid-liquid state.

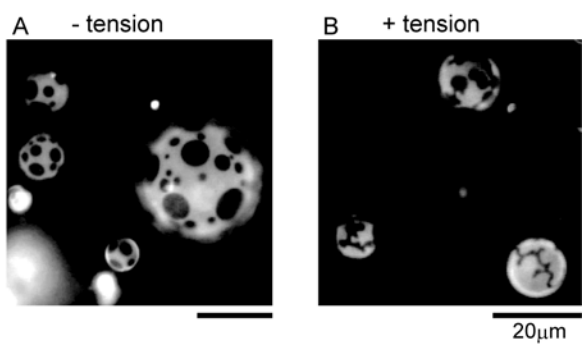

Fig. 6. Tension-induced phase transition from two-liquid to solid-liquid organization. Typical microscopic images of tensionless (A) and tense (B) ternary vesicles of DOPC/DPPC/Chol=40/40/20 at 20 °C. Tense vesicles were under an osmotic pressure of Δ*c*=160mM.

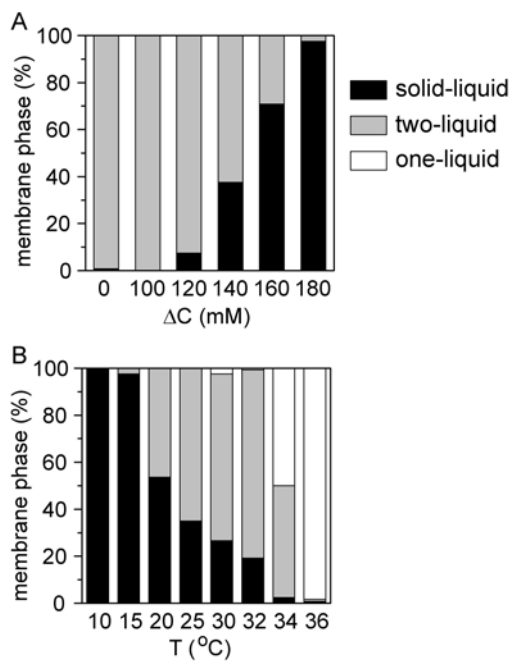

Fig. 7. Probability of membrane phases of a ternary (DOPC/DPPC/Chol=40/40/20) system; (A) as a function of applied osmotic pressure Δ*c* at 15 °C, and (B) as a function of temperature *T* under an osmotic pressure of Δ*c*=180mM. The vesicles were left for 5 min at the desired temperature to equilibrate. A total of 120 vesicles were observed for each condition.

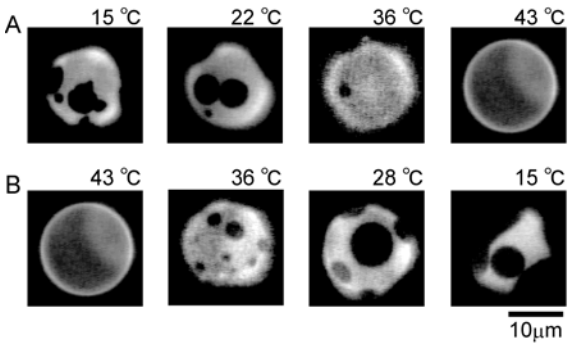

Fig. 8. Microscopic image sequence of membrane phase behavior with a change in temperature between 15 °C and 43 °C. The vesicle is situated under Δc=180mM. The membrane composition is DOPC/DPPC/Chol=40/40/20. Temperature was increased (A) and decreased (B) at 10 °C/min.

We determined the phase diagram of the lateral organization of the ternary DOPC/DPPC/Chol=40/40/20 vesicles as a function of the applied osmotic pressure and temperature (Fig. 9A, also see the Supplementary Information). Low temperature and the application of high pressure result in solid-liquid phase organization. We also examined the phase diagram of membranes with a lower Chol fraction [DOPC/DPPC/Chol=45/45/10 (composition 2 from Fig. 1A)] (Fig. 9B, also see the Supplementary Information). Without tension, the membrane phase of DOPC/DPPC/Chol=45/45/10 is predominantly two-liquid, the same as with DOPC/DPPC/Chol=40/40/20 membranes. However, the phase structure of DOPC/DPPC/Chol=45/45/10 membranes is highly sensitive to the application of osmotic pressure. Solid-liquid phase coexistence is more frequently observed in the pressure-temperature phase diagram of DOPC/DPPC/Chol=45/45/10 than in that of DOPC/DPPC/Chol=40/40/20. At the highest osmotic pressure Δc = 180 mM, DOPC/DPPC/Chol=45/45/10 vesicles showed solid-liquid phase separation independent of temperature, whereas the DOPC/DPPC/Chol=40/40/20 membrane showed two-liquid organization at 25~34 °C. Notably, the miscibility temperature slightly increased under osmotic pressure in both DOPC/DPPC/Chol=40/40/20 and 45/45/10 membranes.

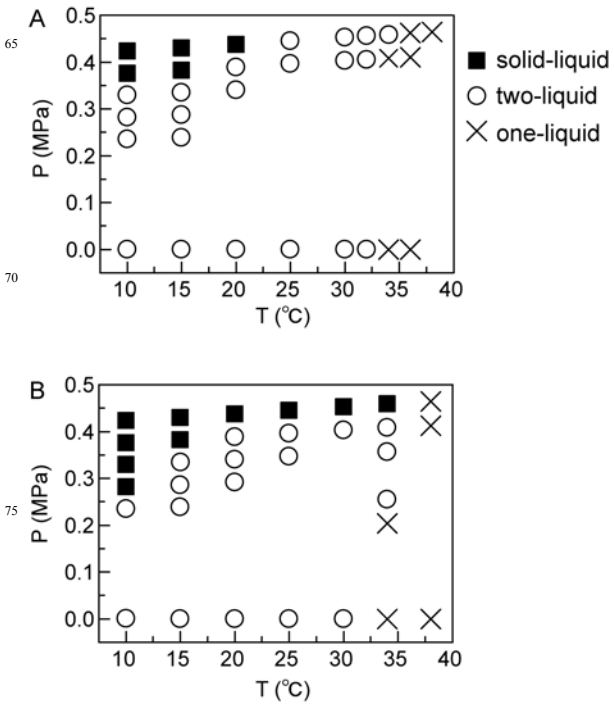

Fig. 9. Phase diagram of membrane lateral organization in ternary vesicles with DOPC/DPPC/Chol=40/40/20 (A) and DOPC/DPPC/Chol=45/45/10 (B). The open circles and filled squares correspond to the situation where two-liquid or solid-liquid phase separation, respectively, is dominant when ≥50 % vesicles show phase separation. Crosses indicate that >50 % vesicles are in a one-liquid (homogenous) state.

Tension-induced phase organization in binary DOPC/DPPC membranes

Next, we investigated phase organization in membranes under pressure with a binary mixture of DOPC and DPPC without Chol (composition 3, 5, 6, 7 and 8 from Fig. 1A). Since membranes without Chol do not have a liquid-order phase, such binary systems can not exhibit two-liquid phase organization, and instead exhibit only solid-liquid phase separation. Figure 10 shows phase diagrams for tense (Δc = 180 mM, black symbol) and tensionless (Δc = 0 mM, gray

symbol) binary membranes with regard to the DOPC/DPPC mixing fraction and temperature. Vesicles with a greater DPPC fraction show a higher miscibility temperature, since the transition temperature of DPPC (42 °C) is higher than that of DOPC (-18 °C). The application of osmotic pressure increased the miscibility temperature for DPPC fractions of 20 % and 80 %. This effect is similar to the results with ternary DOPC/DPPC/Chol membranes, as shown in the phase diagram in Figs. 5 and 9. Therefore, the phase organization induced by membrane tension may be a general property of multi-component membrane systems, since it does not depend on the presence of Chol.

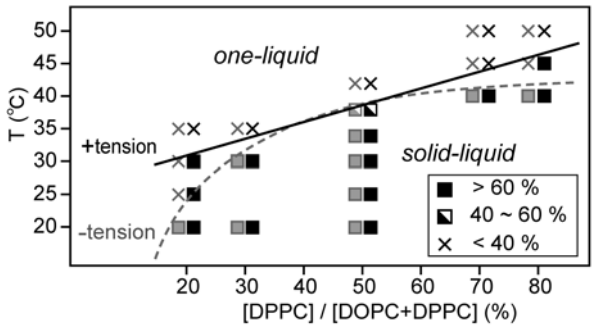

Fig. 10. Phase diagram of the membrane lateral organization in a binary DOPC/DPPC system without Chol. Black and gray symbols indicate tense (Δc=180mM) and tensionless (Δc=0mM) membranes, respectively. The filled and half-filled squares correspond to the situation where >60 % and 40~60 % vesicles exhibit solid-liquid phase separation, respectively. Crosses indicate that <40 % vesicles show phase separation (≥60 % vesicles are in a one-liquid state). The lines show the miscibility boundary (black solid and gray broken lines are with and without tension, respectively).

Tense vesicles do not contain membrane pores as revealed by the measurement of calcein penetration

In addition to the observation of tension-induced membrane phase organization, we confirmed that phase-separated tense vesicles do not have pores within the bilayer. It has been reported that a higher membrane tension may induce the rupture of vesicles due to pore formation.[28] Tension σ can be calculated by eq (1). For vesicles with r = 5 μm (we assume that c_0 = 1/r), P = 0.4 MPa, which corresponds to Δc = 160~180 mM and κ = 10^{-19} J,[5,6] we have σ ~1 Nm^{-1}, which is greater than the rupture tension measured by microcapillary experiments.[29,30] To test the damage in tense membranes, we examined the formation of pores within the bilayer. We adopted a conventional method with the fluorescent molecule calcein (M.W. = 623).[31] Calcein does not penetrate across bilayer membranes. The generation of membrane pores upon the application of external stimuli, such as peptides and surfactants, leads to the penetration of calcein through the bilayer.[31] Therefore, the detection of calcein fluorescence both inside and outside the vesicles would demonstrate the formation of membrane pores. First, we prepared DOPC/DPPC/Chol=40/40/20 vesicles, where calcein existed only outside the vesicles. Figure 11A shows typical microscopic images of a tensionless vesicle; fluorescence from calcein was observed only outside the vesicle, and rho-PE fluorescence of the membrane reflects two-liquid membrane phase organization. After the application of osmotic pressure, although the phase structure shifted from two-liquid to solid-liquid organization, the penetration of calcein was not detected (Fig. 11B). Thus, in our experiments, phase-separated vesicles are stretched without pore formation. This observation without membrane rupture agrees with the experiment of Li and Cheng;[19] they also observed phase-separated giant vesicles under an osmotic pressure of Δc = 100 mM.

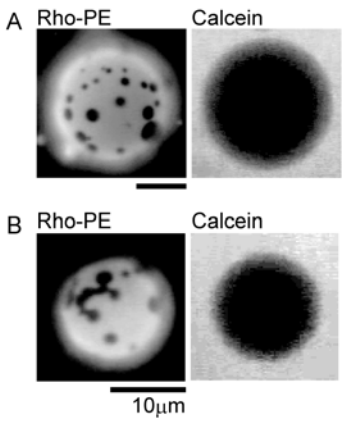

Fig. 11. Test of the leakage of calcein across bilayer membranes under tensionless (A) (Δc=0mM) and tense (B) (Δc=180mM) conditions. The membrane composition is DOPC/DPPC/Chol=40/40/20.

Discussion

The present results show that membrane tension caused changes in the phase structures of multi-component vesicles. At a constant temperature, an external applied tension induced the separation of homogeneous membranes into domains, and two-liquid membranes transitioned to give a state of solid-liquid coexistence with greater ordering. We determined the quantitative phase diagram of the phase organization with regard to the applied osmotic pressure and temperature. This is the first report on the systematic analysis of membrane phase separation under tension. Our results indicate that membrane tension promote phase separation, and this trend agrees with previous experiments.[19,20] Li and Cheng reported that reducing tension by adding a negatively charged lipid eliminates the formation of stripe domains in binary vesicles without Chol.[19] They proposed that repulsive force induced by the lipid charge lowers the attractive interaction among lipid molecules, which leads to the decrease in lateral tension. Additionally, in ternary vesicles with Chol, it was also shown that the presence of a lipid charge decreases the composition region of phase separation.[32,33] Recently, Akimov et al., theoretically suggested that membrane tension increases the line tension between two phases by considering the mismatch of bilayer thickness between two phases.[34] Thus, tense membranes are expected to stabilize phase-separated domains. It has also been reported that a reduction in membrane fluctuation by adhesion promoted phase separation in lipid vesicles.[35]

Here, we used osmotic pressure to produce membrane

tension. Note that we applied osmotic pressure directed toward the outside of vesicles, indicating that water efflux across the membrane increases the inner aqueous volume. After the application of osmotic pressure, the vesicles become completely spherical, which gives the maximum volume per unit area. Further influx stretches the membranes, i.e., the membranes become under tension. Conversely, when osmotic pressure is applied in the opposite direction, such as directed toward the inside of vesicles, water leaves the vesicular space. The decrease in the inner aqueous volume leads to vesicular transformation with membrane curvature, such as budding.[36,37]

Although we obtained the phase diagram of tense membranes with respect to the applied osmotic pressure and temperature, it is difficult to deduce the threshold values of tension to change the phase states. It is because that there are some experimental dispersion of actual tension on the membranes, which is essentially attributed to differences in the area-to-volume ratio of vesicles before osmotic pressure was applied. We should also mention that osmotic stresses applied here is larger than the lysis tension in the literature.[29,30] Although we confirmed that the tense vesicles did not rupture with membrane pores by the measurement of calcein penetration (Fig. 11), the formation of much smaller pores may allow the leakage of glucose molecules to somewhat relieve the applied tension. Further experimental development, such as micropipette aspiration technique,[38-40] intended to specifically estimate membrane tension are underway.

We statistically examined the phase state of vesicle population to obtain the phase diagram at the desired osmotic pressure and temperature (Fig. 5, 9 and 10). In addition, we confirmed the response of a single vesicle to temperature change in Fig. 8: the phase behavior of a tense membrane with a change in temperature at a constant tension. The data from an individual vesicle support the statistical data from vesicle population in a complementary way. Along these lines, we also confirmed the phase behavior of an individual vesicle with a change in tension at a constant temperature (see the Supplementary Information); domains disappeared under the controllable relief of membrane tension.

To better understand the tension-induced bilayer phase organization observed here, we will consider the results of previous monolayer experiments. Many studies have been performed on the lateral segregation of lipid monolayers with a Langmuir trough.[41] Since it is possible to control the molecular area of membrane materials in a monolayer, not only the equation of state but also the phase diagram of multi-component membranes with regard to area and lateral pressure was examined. Stottrup et al., examined the phase separation of ternary DOPC/DPPC/Chol membranes in both bilayer vesicles and a Langmuir monolayer.[42] In their experiments, monolayer phase separation from a one-liquid to two-liquid state was induced when the surface pressure was decreased (molecular area was increased) isothermally. On the other hand, in the bilayer system, molecular area is fixed by the balance between lateral pressure and lipid-water interfacial tension.[15] An external force such as osmotic pressure shifts the balance of force, which leads to a change in lateral pressure and the molecular area. In our experiments, the area-per-lipid increases when the bilayer is stretched by osmotic pressure. The stretched bilayer with a large molecular area tended to show phase separation. Thus, the tension-induced bilayer phase behavior is qualitatively consistent with that in a monolayer system with a controllable area-per-lipid. In addition, with a tense DPPC/Chol membrane, we observed a typical domain structure, called a β region, that has previously been observed in monolayer phase separation (see the Supplementary Information).[42] Without tension, DPPC/Chol bilayer vesicles did not show phase separation, as reported elsewhere.[42] Our observation of domains similar to the β region in tense vesicles suggests that the bilayer phase behavior may be associated with a monolayer phase through a change in thermodynamic variables. Further experimental and theoretical studies are underway to clarify the thermodynamic nature of bilayer phase organization under tension in terms of the assembly of two monolayer systems.

It may be useful to note previous studies on the phase behavior of DOPC/DPPC/Chol membranes under hydrostatic pressure, although osmotic and hydrostatic pressure have different effects on vesicle membranes. Osmotic pressure directed toward the outside of vesicles leads to membrane stretching, i.e., lateral tension, whereas hydrostatic pressure changes the density of the total lipid-water system. Jeworrek et al., reported the transition from a one-liquid phase to two-liquid phase separation under the application of hydrostatic pressure of ~10^2 MPs, using Fourier transform infrared (FTIR) spectroscopy.[43,44] In their experiments, as the applied hydrostatic pressure increased, solid-liquid phase separation emerged. This effect of hydrostatic pressure is similar to that with osmotic pressure in our results.

Conclusion

We studied the effect of membrane tension on lateral phase organization within bilayer vesicles. Membrane tension was controlled by the application of osmotic pressure. We obtained a phase diagram of DOPC/DPPC/Chol membranes as a function of the applied osmotic pressure and temperature. We found that membrane tension induced phase separation in homogeneous membranes. In addition, when two-liquid membranes were put under tension, the phase structures changed to give a state of solid-liquid coexistence. With actual plasma membranes, lateral tension induced by the application of mechanical forces has been reported to cause changes in the conformation of embedded peptides/proteins that regulate signal transductions.[45-47] To quantify the membrane structural dynamics under tension, molecular dynamics (MD) simulations have also been developed.[48,49] Our findings may provide insight into the biophysics of bilayer phase organization under tension.

Acknowledgements

We thank Prof. Takashi Taniguchi (Kyoto Univ.), Prof. Shigeyuki Komura (Tokyo Metropolitan Univ.), Prof. Masayuki Imai and Dr. Yuka Sakuma (Ochanomizu Univ.) for their fruitful discussions. This work was supported by a

KAKENHI Grant-in-Aid for Scientific Research B (Grant No. 20360370) from JSPS, on Priority Areas "Soft Matter Physics" and "Bio Manipulation" from MEXT of Japan, and by a Sunbor Grant from the Suntory Institute for Bioorganic Research.

Notes and references

[a] *School of Materials Science, Japan Advanced Institute of Science and Technology, 1-1 Asahidai, Nomi, Ishikawa 923-1292, Japan, Tel: +81-761-51-1657; E-mail: t-hamada@jaist.ac.jp*

[b] *Graduate School of Engineering, Osaka City University, 3-3-138 Sugimoto, Sumiyoshi-ku, Osaka 558-8585, Japan*

† Electronic Supplementary Information (ESI) available: Percentage of phase-separated vesicles in each condition, domain structure in DPPC/Chol binary membranes, and relief of membrane tension in a single vesicle. See DOI: 10.1039/b000000x/

1. D. Lingwood and K. Simons, *Science*, 2010, **327**, 46.
2. K. Simons and E. Ikonen, *Nature,* 1997, **387**, 569.
3. D. A. Brown and E. London, *J. Biol. Chem*, 2000, **275**, 17221.
4. J. F. Hancock, *Nat. Rev. Mol. Cell Biol.*, 2006, **7**, 456.
5. R. Lipowsky and R. Dimova, *J. Phys.: Cond. Mat.,* 2003, **15**, S31.
6. T. Baumgart, S. T. Hess and W. W. Webb, *Nature,* 2003, **425**, 821.
7. S. L. Veatch and S. L. Keller, *Biochim. Biophys. Acta, Mol. Cell Res.,* 2005, **1746**, 172.
8. L. Bagotolli and P. B. S. Kumar, *Soft Matter*, 2009, **5**, 3234.
9. N. F. Morales-Penningston, J. Wu, E. R. Farkas, S. L. Goh, T. M. Konyakhina, J. Y. Zheng, W. W. Webb and G. W. Feigenson, *Biochim. Biophys. Acta, Biomembr.,* 2010, **1798**, 1324.
10. S. L. Veatch and S. L. Keller, *Phys. Rev. Lett.,* 2002, 89, 268101.
11. S. L. Veatch and S. L. Keller, *Biophys J,* 2003, **85**, 3074.
12. T. Hamada, R. Sugimoto, T. Nagasaki and M. Takagi, *Soft Matter,* 2011, 7, 220.
13. S. L. Keller, T. G. Anderson and H. M. McConnell, *Biophys. J.,* 2000, **79**, 2033.
14. B. Lin, M. C. Shih, T. M. Bohanon, G. E. Ice and P. Dutta, *Phys. Rev. Lett.,* 1990, **65**, 191.
15. N. K. Adam, *The Physics and Chemistry of Surfaces*, Clarendon Press, Oxford, U.K., 1938.
16. M. A. Lomholt, B. Loubet and J. H. Ipsen, *Phys. Rev. E Stat. Nonlin. Soft Matter Phys,* 2011, **83**, 011913.
17. S. Rozovsky, Y. Kaizuka and J. T. Groves, *J. Am. Chem. Soc.,* 2005, **127**, 36.
18. S. Komura, N. Shimokawa and D. Andelman, *Langmuir,* 2006, **22**, 6771.
19. L. Li and J.-X. Cheng, *Biochemistry,* 2006, **45**, 11819.
20. A. G. Ayuyan and F. S. Cohen, *Biophys. J.*, 2008, **94**, 2654.
21. O.-Y. Zhong-can and W. Helfrich, *Phys. Rev. Lett.*, 1987, **59**, 2486.
22. P., Walde, K. Cosentino, H. Engel and P. Stano, *ChemBioChem*, 2010, **11**, 848.
23. U. Seifert, *Adv. Phys.,* 1997, **46**, 13.
24. P. Ziherl and S. Svetina, *Europhys. Lett.,* 2005, **70**, 690.
25. J. Majhenc, B. Božič, S. Svetina and B. Žekš, *Biochim. Biophys. Acta, Biomembr.,* 2004, **1664**, 257.
26. K. Ishii, T. Hamada, M. Hatakeyama, R. Sugimoto, T. Nagasaki and M. Takagi, *ChemBioChem,* 2009, **10**, 251.
27. D. Saeki, T. Hamada and K. Yoshikawa, *J. Phys. Soc. Jpn.,* 2006, **75**, 013602.
28. Y. Levin and M. A. Idiart, *Physica A,*2004, **331**, 571.
29. J. D. Moroz and P. Nelson, *Biophys. J.,* 1997, **72**, 2211.
30. E. Evans, V. Heinrich, F. Ludwig and W. Rawicz, *Biophys. J.,* 2003, **85**, 2342.
31. Y. Tamba and M. Yamazaki, *J. Phys. Chem. B*, 2009, **113**, 4846.
32. C. C. Vequi-Suplicy, K. A. Riske, R. L. Knorr and R. Dimova, *Biochim. Biophys. Acta, Biomembr.,* 2010, **1798**, 1338.
33. N. Shimokawa, M. Hishida, H. Seto and K. Yoshikawa, *Chem. Phys. Lett.*, 2010, **496**, 59.
34. S. A. Akimov, P. I. Kuzmin, J. Zimmerberg and F. S. Cohen, *Phys. Rev. E Stat. Nonlin. Soft Matter Phys.,* 2007, **75**, 011919.
35. V. D. Gordon, M. Deserno, C. M. J. Andrew, S. U. Egelhaaf and W. C. K. Poon, *Europhys. Lett.,* 2008, **84**, 48003.
36. T. Hamada, Y. Miura, K. Ishii, S. Araki, K. Yoshikawa, M. Vestergaard and M. Takagi, *J. Phys. Chem. B*., 2007, **111**, 10853.
37. L. Li, X. Liang, M. Lin, F. Qiu and Y. Yang, *J. Am. Chem. Soc.*, 2005, **127**, 17996.
38. E. Evans and W. Rawicz, *Phys. Rev . Lett.*, 1990, **64**, 2094.
39. A. Tian, C. Johnson, W. Wang and T. Baumgart, *Phys. Rev. Lett.*, 2007, **98**, 208102.
40. Y. Li, R. Lipowsky and R. Dimova, *Proc. Natl. Acad. Sci. USA,* 2011, **108**, 4731.
41. H. M. McConnell and A. Radhakrishnan, *Biochim. Biophys. Acta, Biomembr.*, 2003, **1610**, 159.
42. B. L. Stottrup, D. S. Stevens and S. L. Keller, *Biophys. J.,* 2005, **88**, 269.
43. C. Jeworrek, M. Pühse and R. Winter, *Langmuir,* 2008, **24**, 11851.
44. R. Winter and C. Jeworrek, *Soft Matter,* 2009, **5**, 3157.
45. M. Goulian, O. N. Mesquita, D. K. Fygenson, C. Nielsen, O. S. Andersen and A. Libchaber, *Biophys. J.,* 1998, **74**, 328.
46. M. Chachisvilis, Y.-L. Zhang and J. A. Frangos, *Proc. Natl. Acad. Sci. USA,* 2006, **103**, 15463.
47. J. A. Lundbak, S. A. Collingwood, H. I. Ingólfsson, R. Kapoor and O. S. Andersen, *J. R. Soc. Interface*, 2010, **7**, 373.
48. J. C. Shillcock and R. Lipowsky, *Nature Materials,* 2005, **4**, 225.
49. H. S. Muddana, R. R. Gullapalli, E. Manias and P. J. Butler, *Phys. Chem. Chem. Phys.,* 2011, **13**, 1368.